# On the statistical properties of the widths of the mean radio pulsar profiles

(a connection with the orthogonal emission modes)

A. Yu. Istomin[2,1], F. A. Kniazev[2,1], V. S. Beskin[1,2]

*[1] - Lebedev Physical Institute*
*[2] -Moscow Institute of Physics and Technology*

*HEACOSS — 2026*

# Isolated radio pulsars

## Radiopulsar:

- is a neutron star
- has a magnetic filed ~ $10^{12}$ G
- emit in radio band above its magnetic poles
- is observed as periodic pulses due to «lighthouse effect»

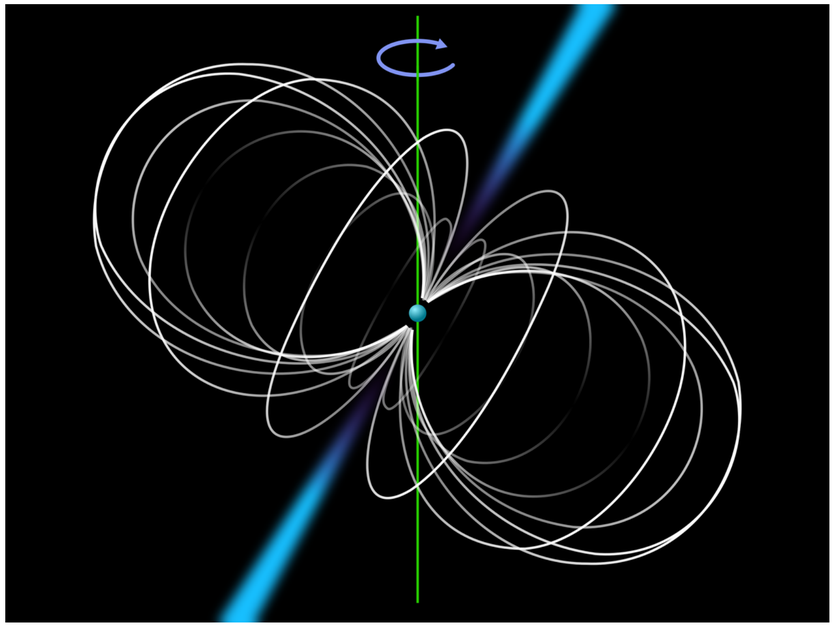

A cartoon of radio pulsar

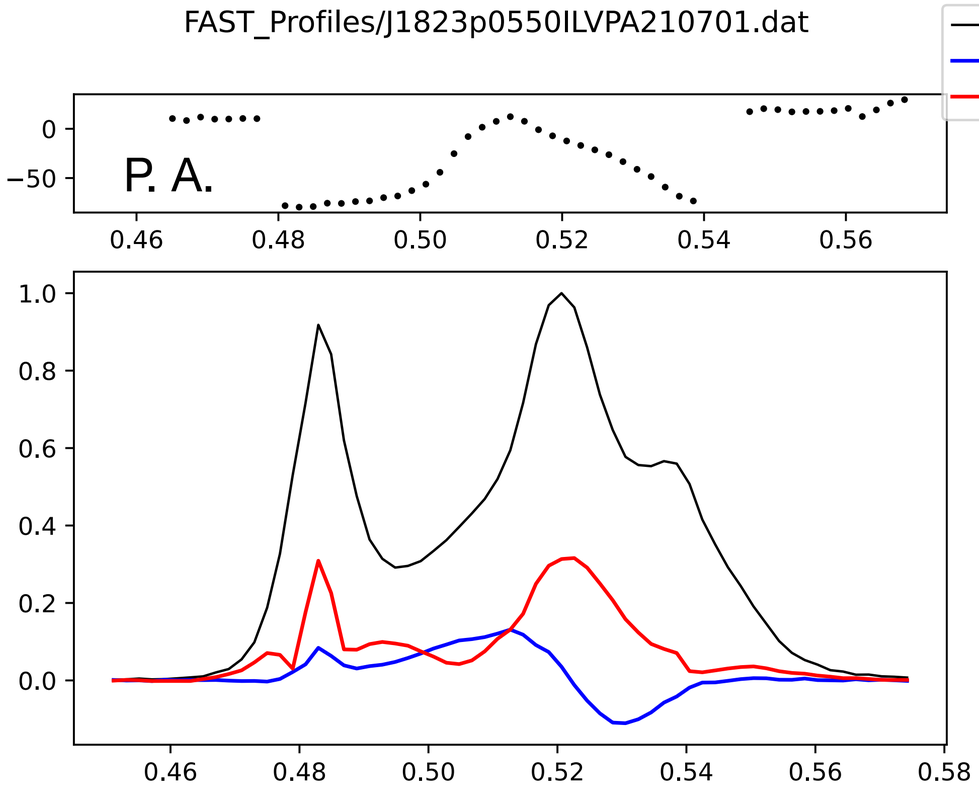


An example of mean intensity and polarisation profile

*Wang et. al., 2023*

# Mean intensity profiles

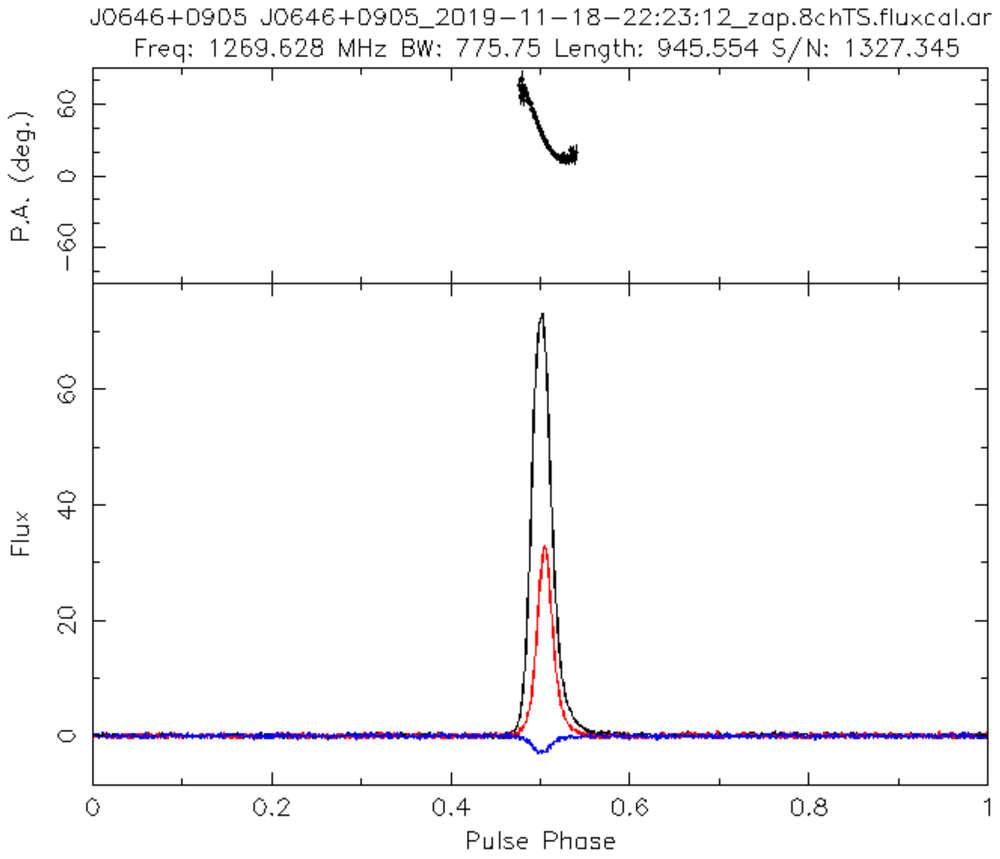


Single-humped intensity profile

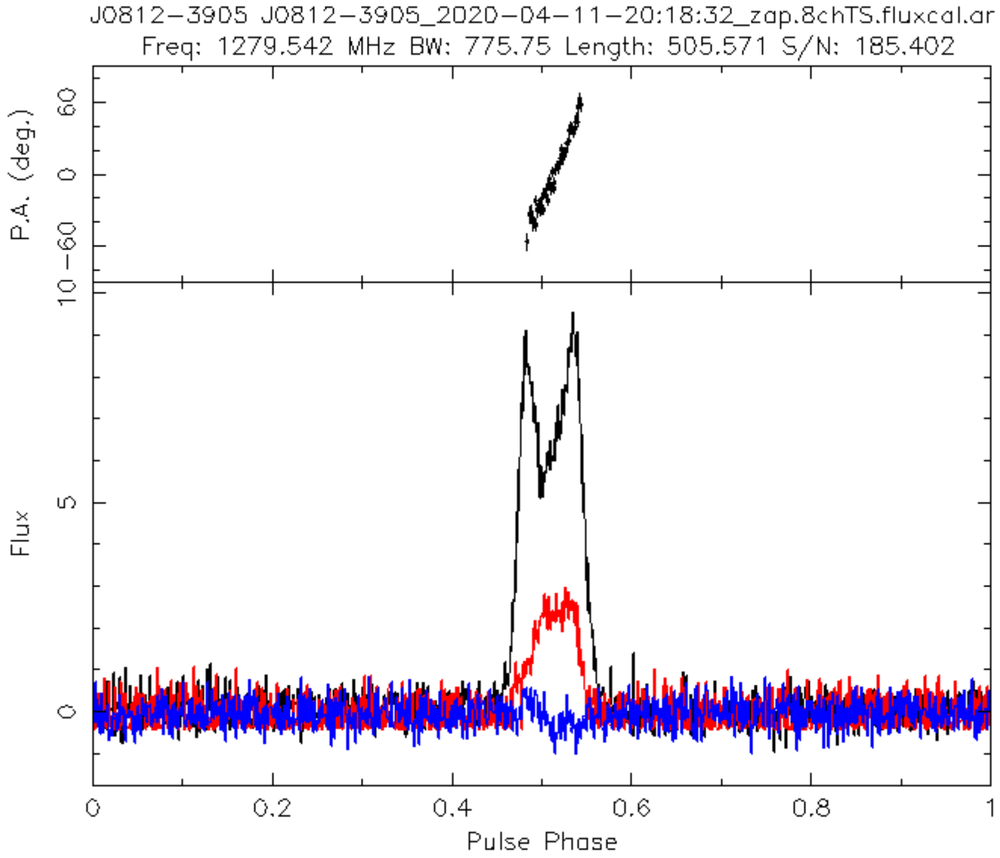


Double-humped intensity profile

*Data from B. Posselt et. al., 2023*

# Orthogonal emission modes—observations

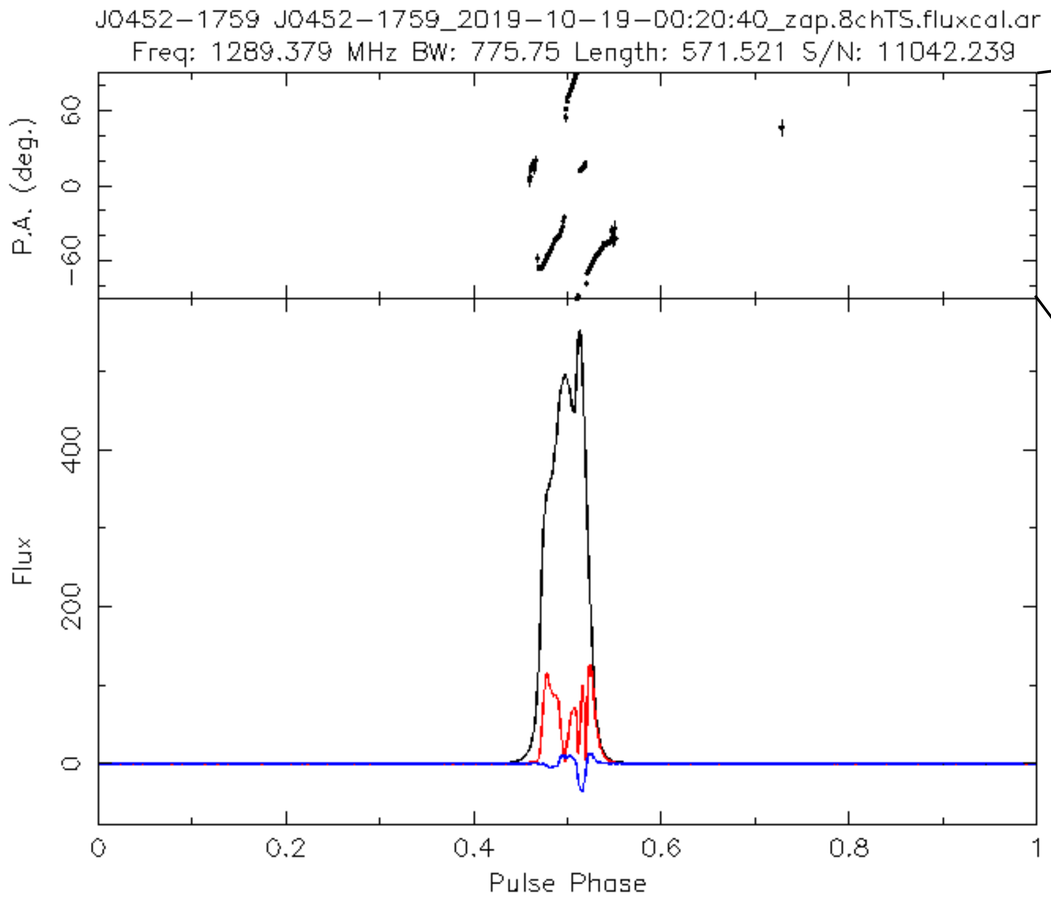


*B. Posselt et. al., 2023*

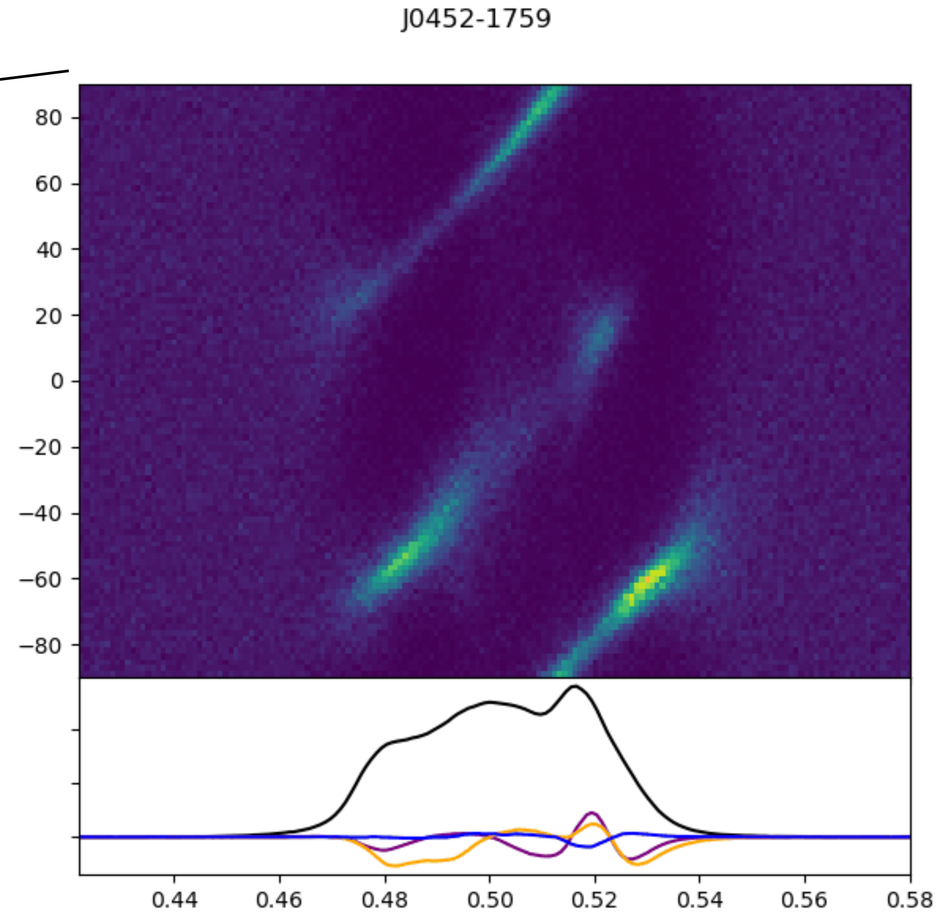


*Keith et al., 2026*

# Orthogonal emission modes—observations

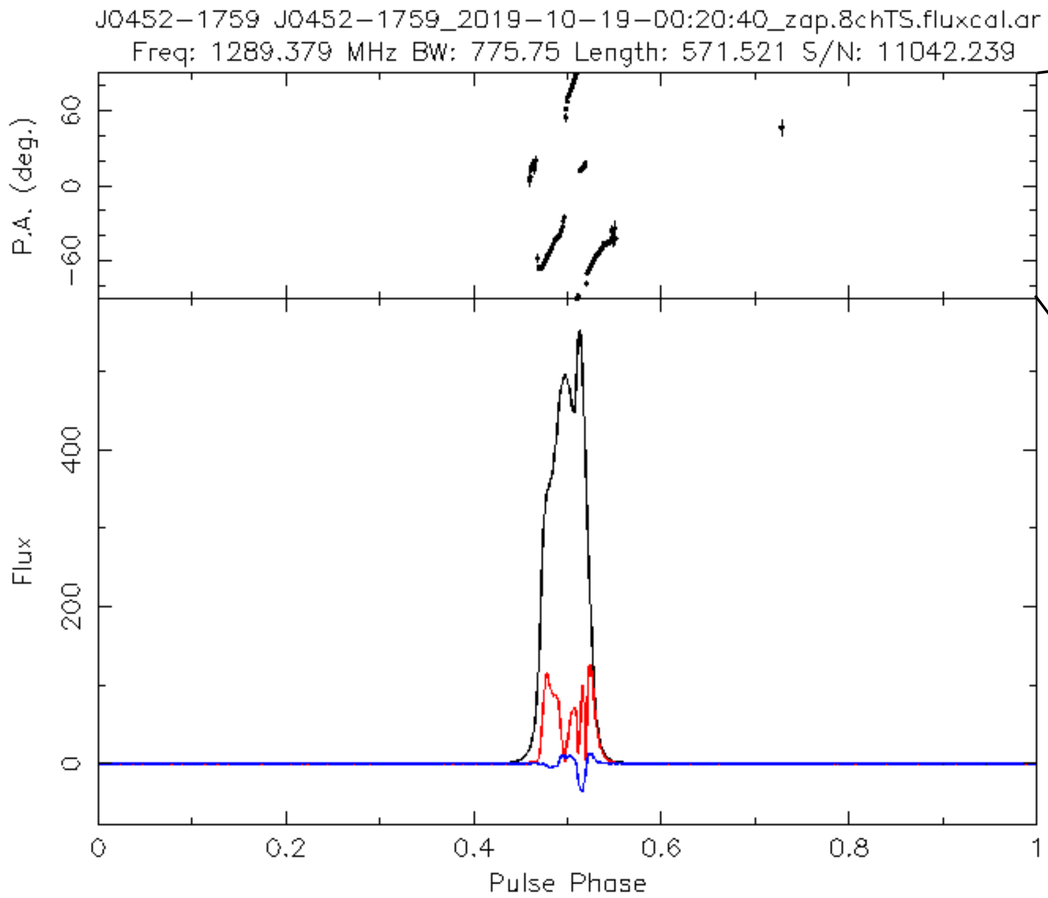


*B. Posselt et. al., 2023*

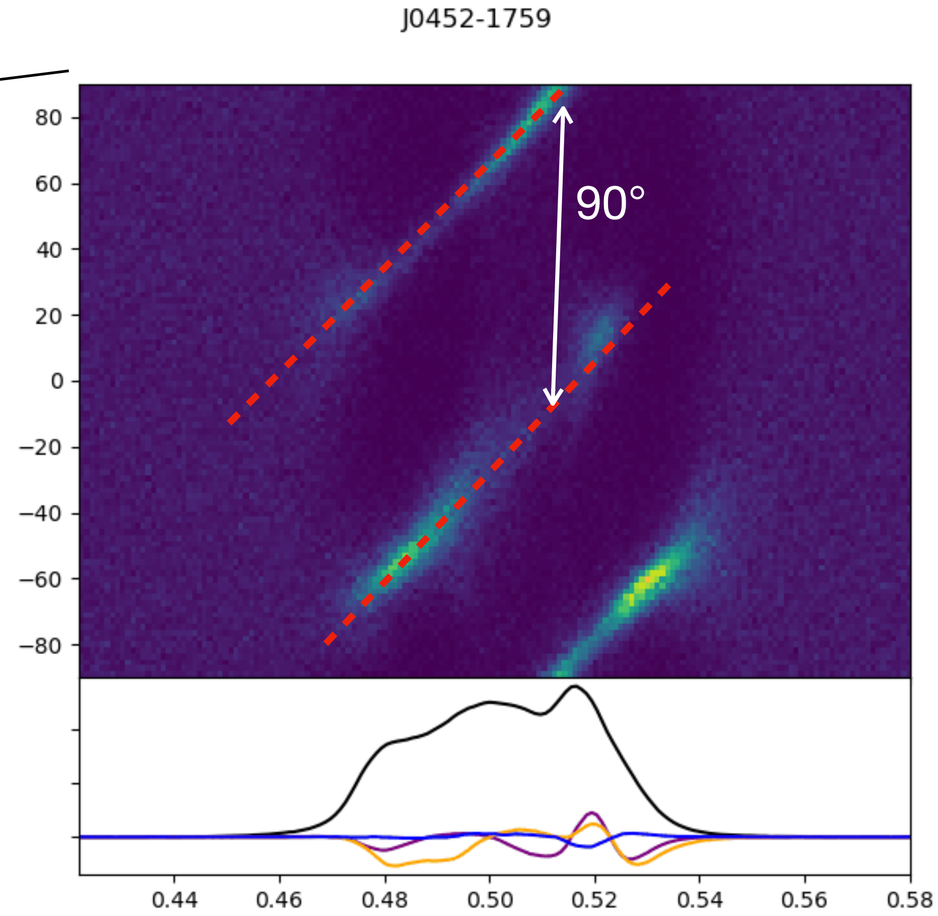


*Keith et al., 2026*

# Orthogonal emission modes— theory

Two orthogonal modes — **O** (ordinary) and **X** (extraordinary)

$$n_O \approx 1 + \frac{\theta_b^2}{4} - \left( \left\langle \frac{\omega_{\mathrm{pe}}^2}{\gamma^3 \omega^2} \right\rangle + \frac{\theta_b^4}{16} \right)^{1/2}$$

$$n_X = 1$$

**O**-mode — electric field vector lies in **(k, B)** plane

**X**-mode — electric field vector is perpendicular to **(k, B)** plane

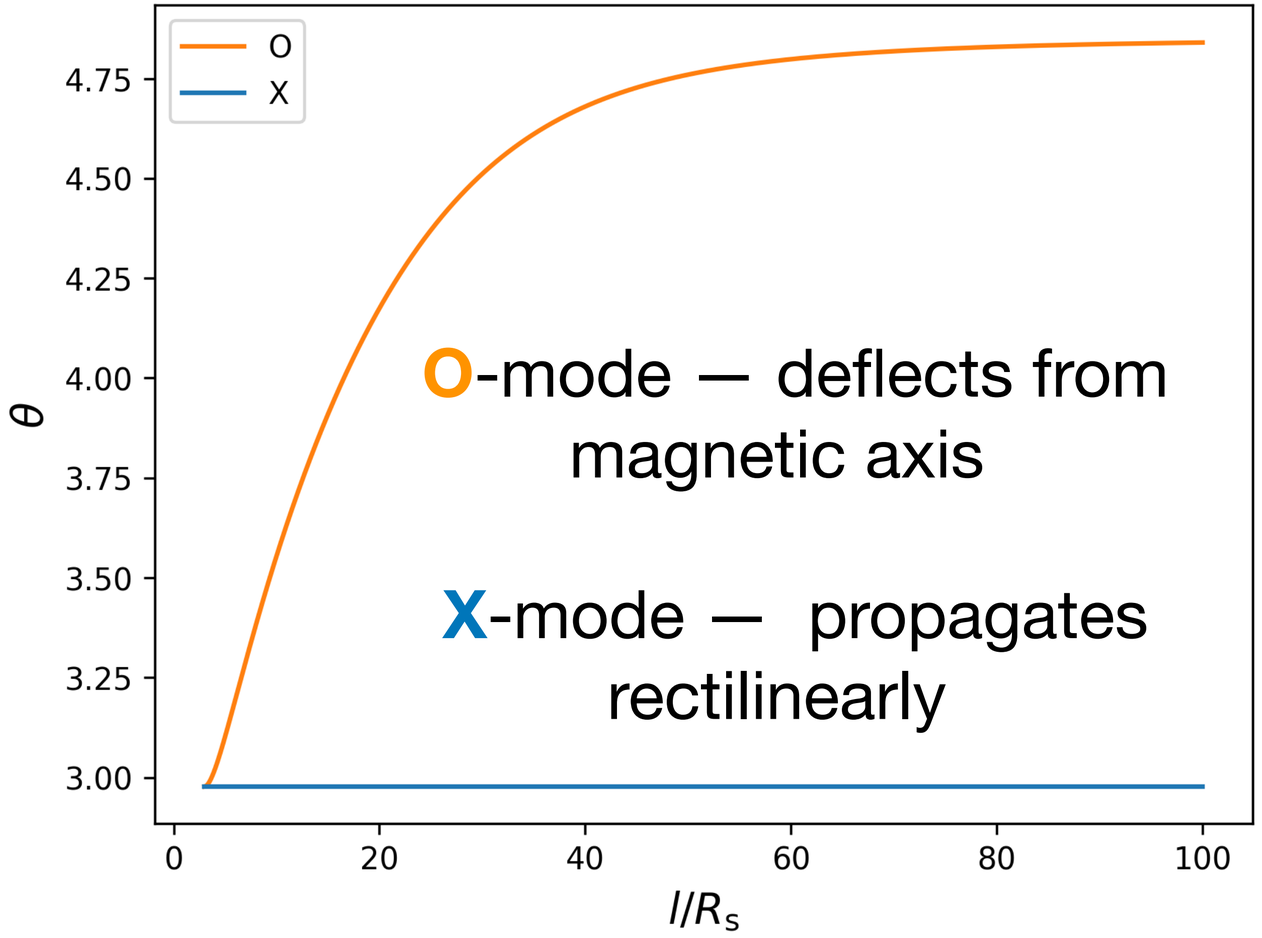

# Orthogonal emission modes—predictions

**O**-mode — usually creates double-humped mean intensity profiles, which are on average wider

**X**-mode — usually creates single-humped mean intensity profiles, which are on average narrower

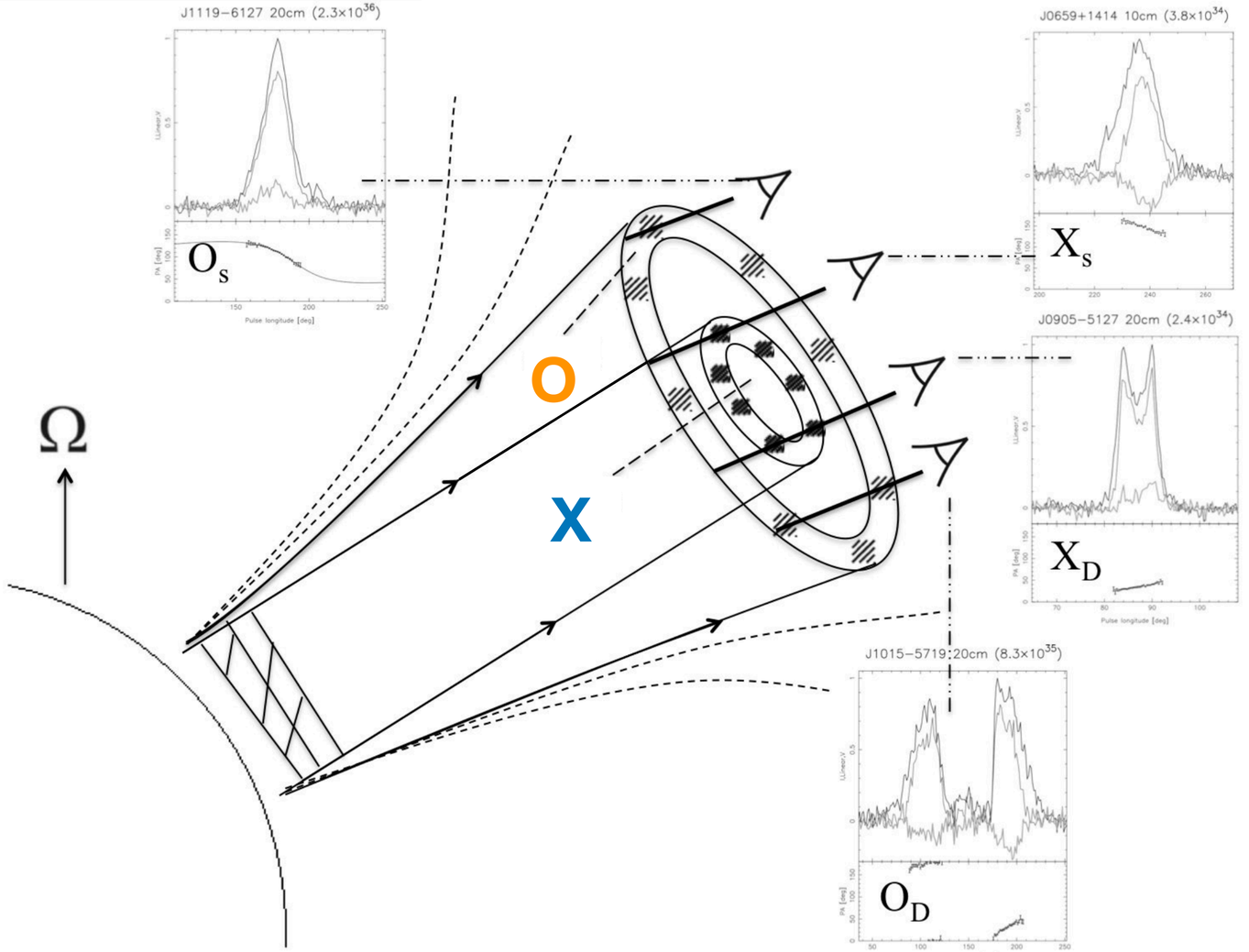


*Beskin V. S., Philippov A. A, MNRAS, 425, 2, 814 (2012)*

# Dominant mode identification — theory

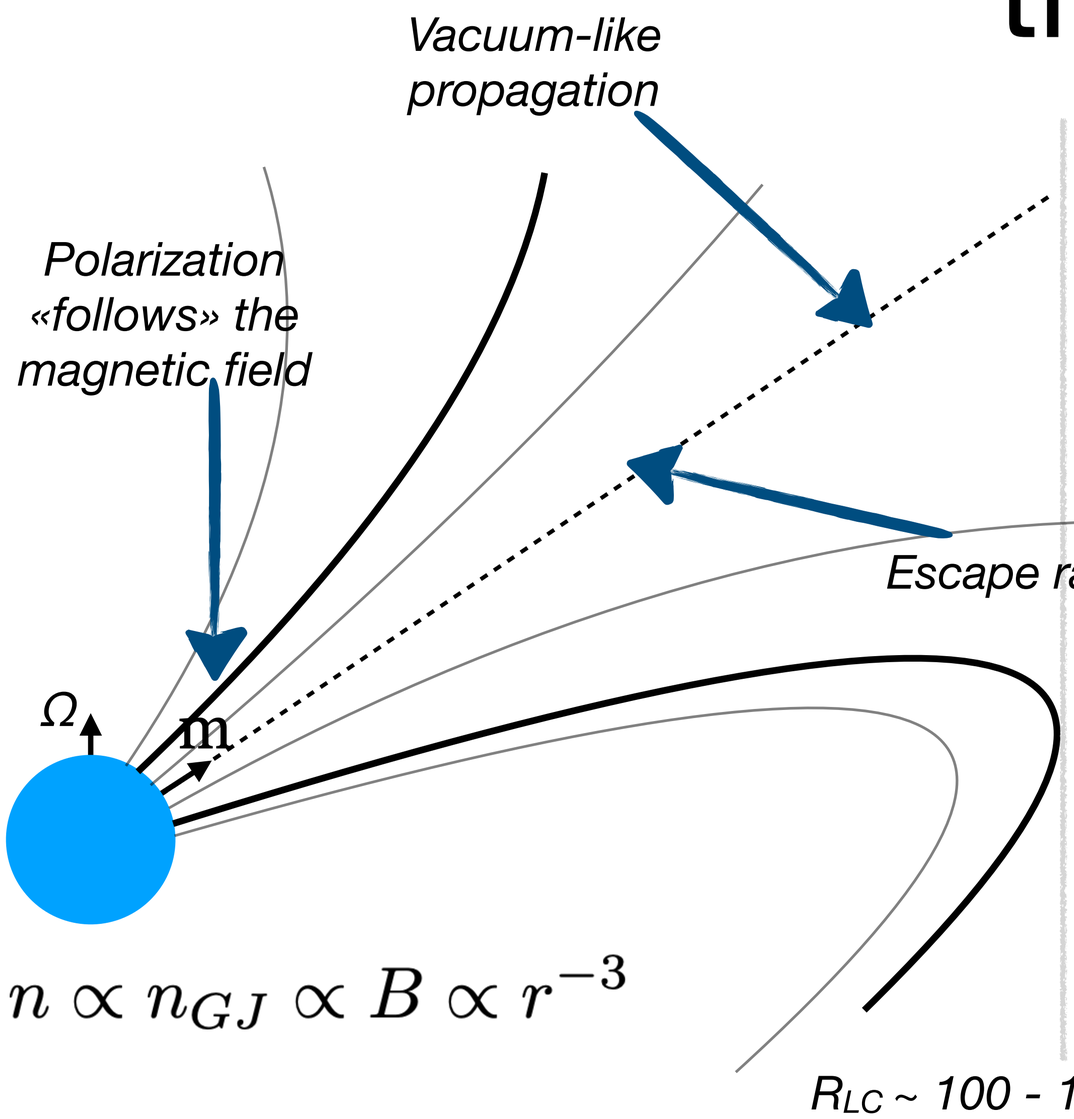


*Kravtsov-Orlov equations*

*Kravtsov Yu.A. & Orlov Yu.I. (1990)*

$$\frac{\mathrm{d}\Theta_1}{\mathrm{d}l} = \frac{\omega}{2c}\mathrm{Im}\left[\varepsilon_{x'y'}\right] - \frac{1}{2}\frac{\omega}{c}\Lambda\cos[2\Theta_1 - 2\beta_B(l) - 2\delta(l)]\sinh 2\Theta_2,$$

$$\frac{\mathrm{d}\Theta_2}{\mathrm{d}l} = \frac{1}{2}\frac{\omega}{c}\Lambda\sin[2\Theta_1 - 2\beta_B(l) - 2\delta(l)]\cosh 2\Theta_2.$$

Circular polarization is connected with the P. A. evolution

*Lyubarskii, Y. E. & Petrova, S. A. (1998)*

*Philippov, A. A. & Beskin, V. S. (2012)*

*Hakobyan, H. L., Beskin V. S., Philippov A. A. (2016)*

# Dominant mode identification — procedure

From the emission transfer equations analysis (Kravtsov-Orlov equations):

**O**-mode — signs of circular polarisation and position angle derivative are opposite

**X**-mode — signs of circular polarisation and position angle derivative are the same

*A. S. Andrianov, V. S. Beskin, 2010*
*V. S. Beskin, A. A. Philippov, 2012*

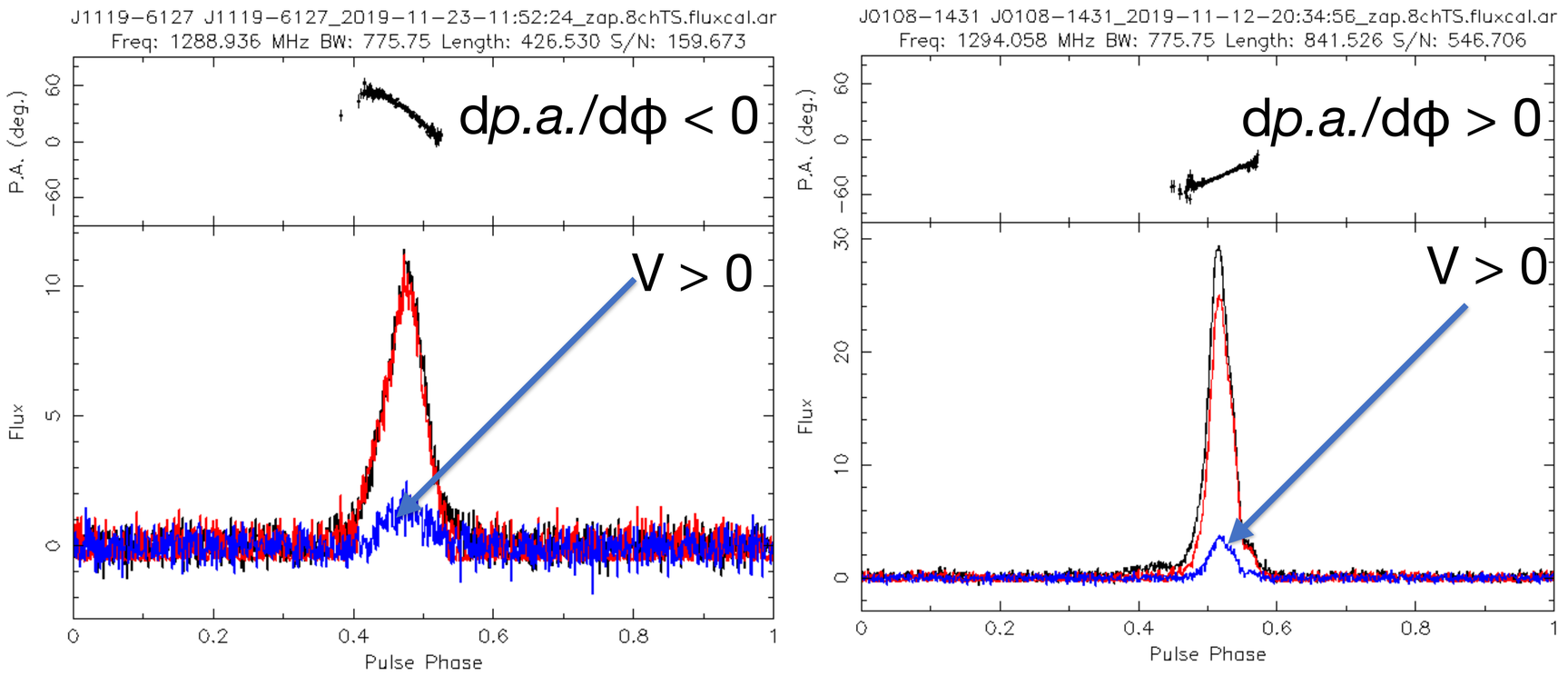


**O** - mode

**X** - mode

Identification of the dominant emission mode. The data is taken from *B. Posselt et. al., 2023*

# FAST and MeerKAT data

FAST

*Wang, S. Q., Wang, J. B., Li, D. Z., et al., RAA, 23, 104002 (2023)*

MeerKAT

*B. Posselt et. al., MNRAS, 520, 4582 (2023)*

# FAST and MeerKAT data

**Abstract**

Pulsar polarization profiles form a very basic database for understanding the emission processes in a pulsar magnetosphere. After careful polarization calibration of the 19-beam *L*-band receiver and verification of beam-offset observation results, we obtain polarization profiles of 682 pulsars from observations by the Five-hundred-meter Aperture Spherical radio Telescope (FAST) during the Galactic Plane Pulsar Snapshot survey and other normal FAST projects. Among them, polarization profiles of about 460 pulsars are observed for the first time. The profiles exhibit diverse features. Some pulsars have a polarization position angle curve with a good S-shaped swing, some with orthogonal modes; some have components with highly linearly po
circularly polarized components; some have a very wide profile, coming from an alig
interpulse from a perpendicular rotator; some wide profiles are caused by inter
geometric parameters for 190 pulsars from the S-shaped position angle curves or wit
that the linear and circular polarization or the widths of pulse profiles have various fre
with a large fraction of linear polarization are more likely to have a large Edot.

FAST

*Wang, S. Q., Wang, J. B., Li, D. Z., et al., RAA, 23, 104002 (2023)*

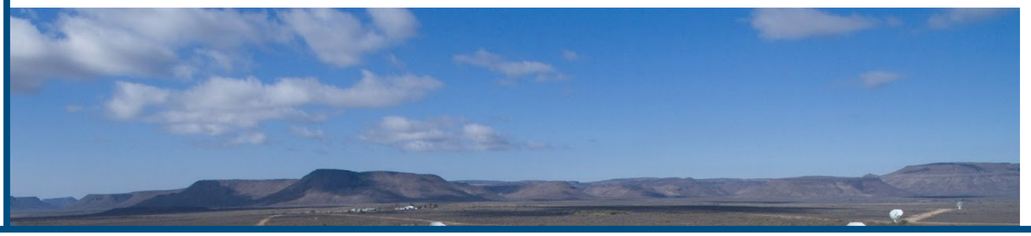

**ABSTRACT**

We present the largest single survey to date of average profiles of radio pulsars, observed and processed using the same telescope and data reduction software. Specifically, we present measurements for 1170 pulsars, observed by the Thousand Pulsar Array programme at the 64-dish SARAO MeerKAT radio telescope, in a frequency band from 856 to 1712 MHz. We provide rotation measures (RM), dispersion measures, flux densities, and polarization properties. The catalogue includes 254 new RMs that substantially increase the total number of known pulsar RMs. Our integration times typically span over 1000 individual rotations per source. We show that the radio (pseudo-) luminosity has a strong, shallow dependence on the spin-down energy, proportional to $\dot{E}^{0.15\pm0.04}$, that contradicts some previous proposals of population synthesis studies. In addition, we find a significant correlation between the steepness of the observed flux density spectra and $\dot{E}$, and correlations of the fractional linear polarization with $\dot{E}$, the spectral index, and the pulse width, which we discuss in the context of what is known about pulsar radio emission and how pulsars evolve with time. On the whole, we do not see significant correlations with the estimated surface magnetic field strength, and the correlations with $\dot{E}$ are much stronger than those with the characteristic age. This finding lends support to the suggestion that magnetic dipole braking may not be the dominant factor for the evolution of pulsar rotation over the lifetimes of pulsars. A public data release of the high-fidelity time-averaged pulse profiles in full polarization accompanies our catalogue.

MeerKAT

*B. Posselt et. al., MNRAS, 520, 4582 (2023)*

# Subsamples

## Selection criteria:

- High singal-to-noise ratio
- Single-humped or double-humped profile
- Monotonous P.A. profile
- Only one dominant emission mode (no orthogonal jumps)
- Not a millisecond pulsar

FAST: 114/682 pulsars

MeerKAT: 421/1270 pulsars

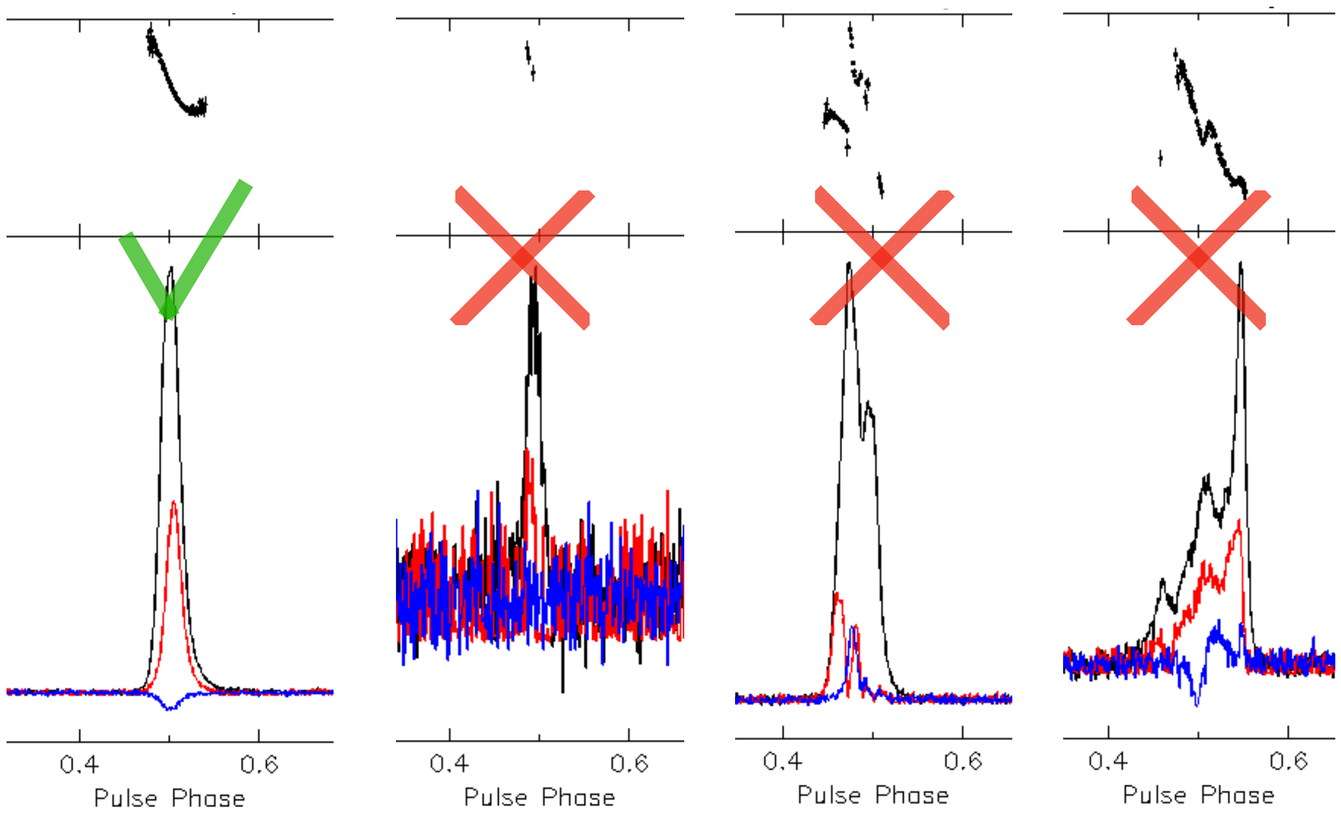


*B. Posselt et. al. (2023)*

# Widths of the mean intensity profiles

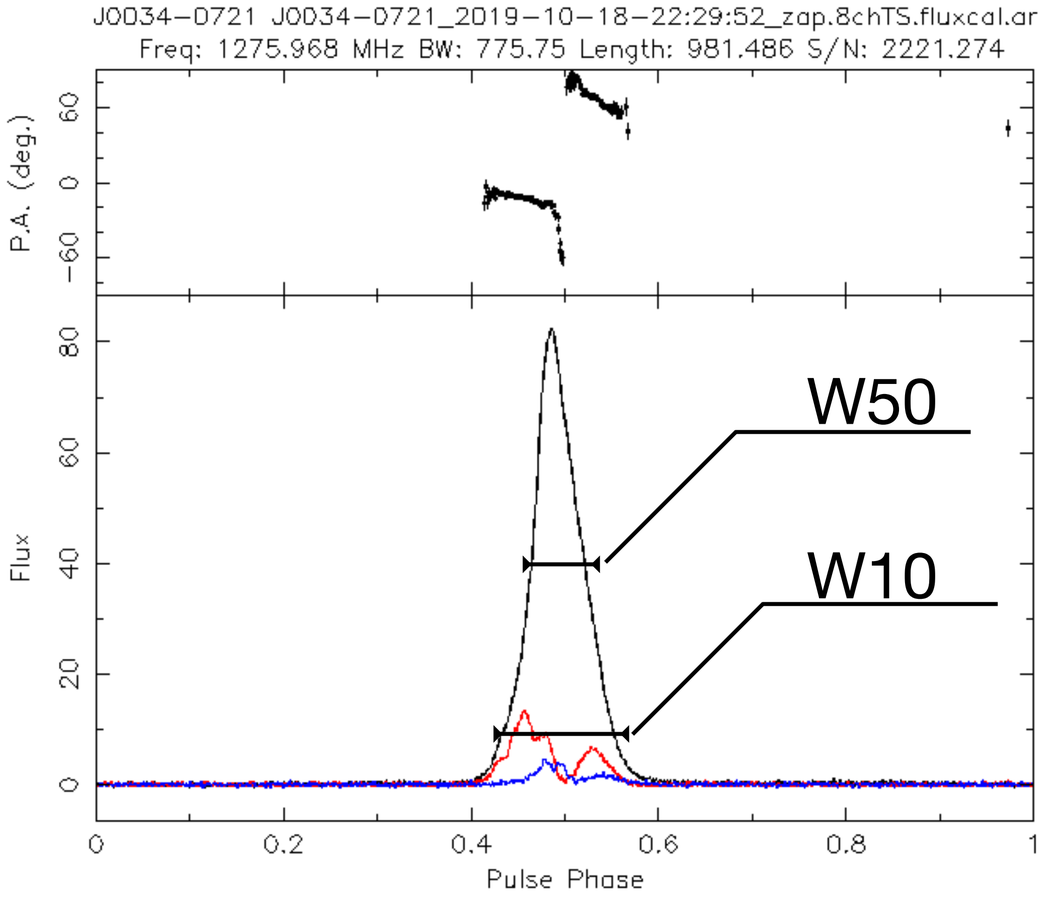


*B. Posselt et. al. (2023)*

WX — profile width on X% level with respect to the peak intensity

Caveats:

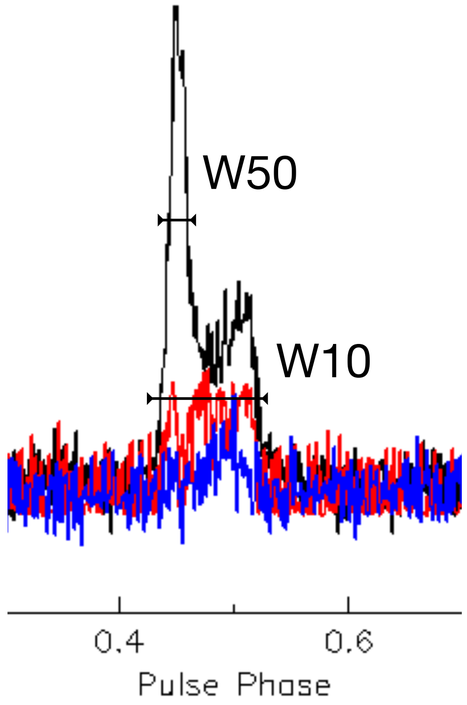


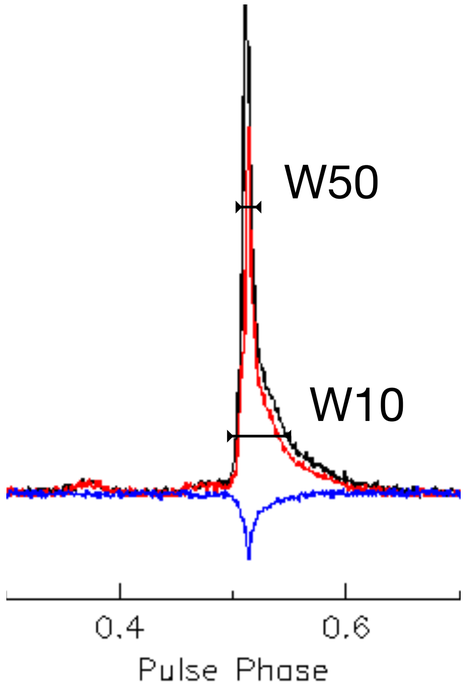

# Normalised profile widths distributions

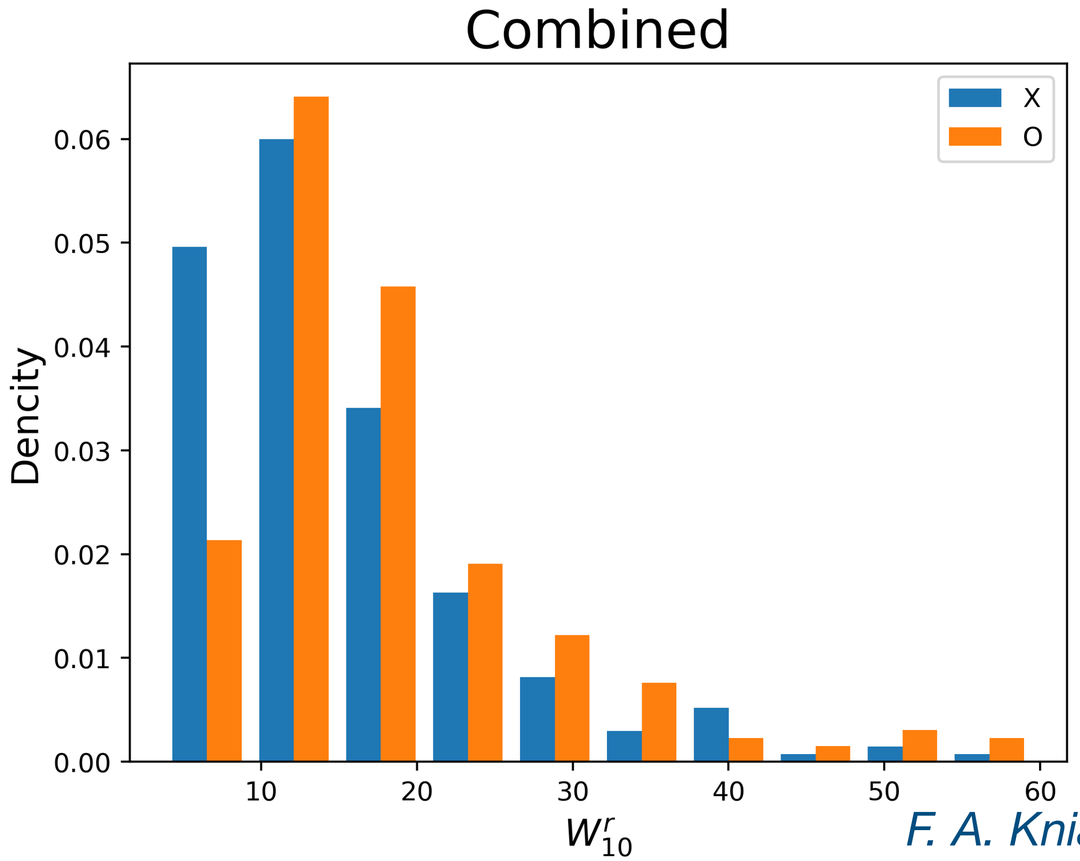


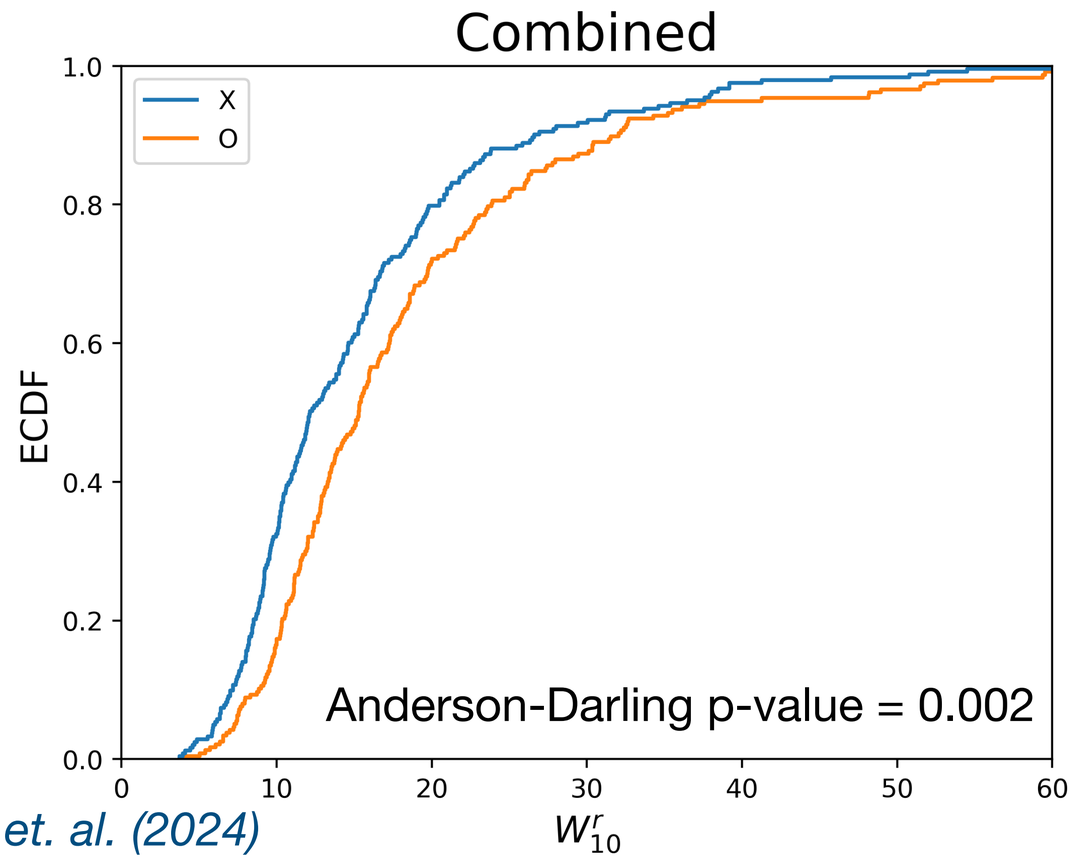


*F. A. Kniazev et. al. (2024)*

| | N = **Xs**+**Xd**+**Os**+**Od** | Xs | Xd | Os | Od | $X_{tot}$ | $O_{tot}$ |
|---|---|---|---|---|---|---|---|
| FAST | $39+19+19+37=114$ | $12.4^{+2.4}_{-2.6}$ | $12.7^{+5.7}_{-3.3}$ | $12.6^{+6.1}_{-1.5}$ | $16.0^{+2.7}_{-2.3}$ | $12.5^{+2.3}_{-2.2}$ | $15.4^{+2.5}_{-2.2}$ |
| MeerKAT | $178+36+93+114=421$ | $10.2^{+1.4}_{-0.7}$ | $11.6^{+2.9}_{-1.6}$ | $12.9^{+1.9}_{-1.1}$ | $16.8^{+2.0}_{-1.5}$ | $10.6^{+1.1}_{-0.9}$ | $15.3^{+0.8}_{-1.8}$ |

# Conclusions

- The procedure of mode identification allowed splitting the pulsar sample into two subsamples with different statistical properties
- Double-humped profiles are more frequently formed by the O-mode, while single-humped by the X-mode
- Mean intensity profiles formed by the O-mode are on average wider than profiles, formed by the X-mode

# Widths of the mean intensity profiles

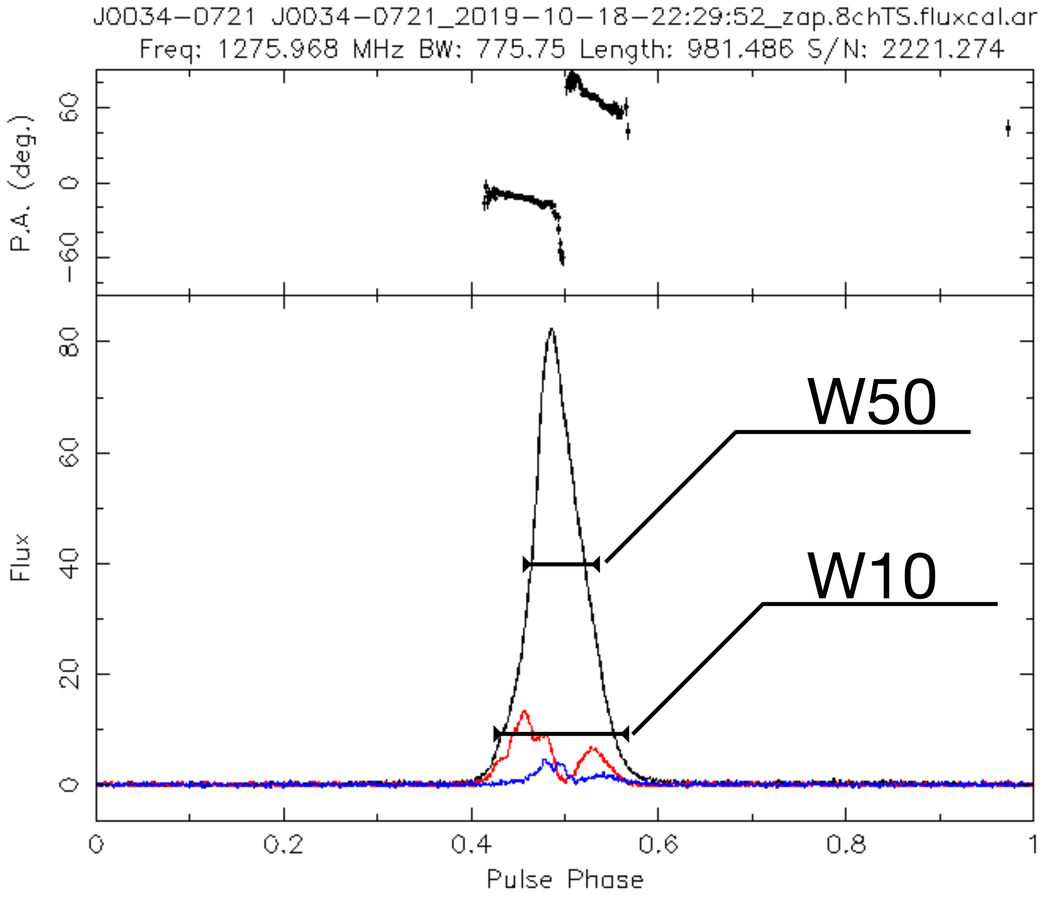


*B. Posselt et. al. (2023)*

$$W_{\rm obs} = \frac{2\rho_0}{\sin\chi}\left(1-\left(\frac{\beta}{\rho_0}\right)^2\right)^{1/2} \equiv \frac{W_0}{\sin\chi}(1-x^2)^{1/2}$$

WX - profile width on X% level with respect to peak intensity

$$W_0^{\rm O} \approx 11.8^\circ P^{-0.49}$$

$$W_0^{\rm X} \approx 6.9^\circ P^{-0.33}$$

$$W^{\rm r} = W_{\rm obs} P^q$$

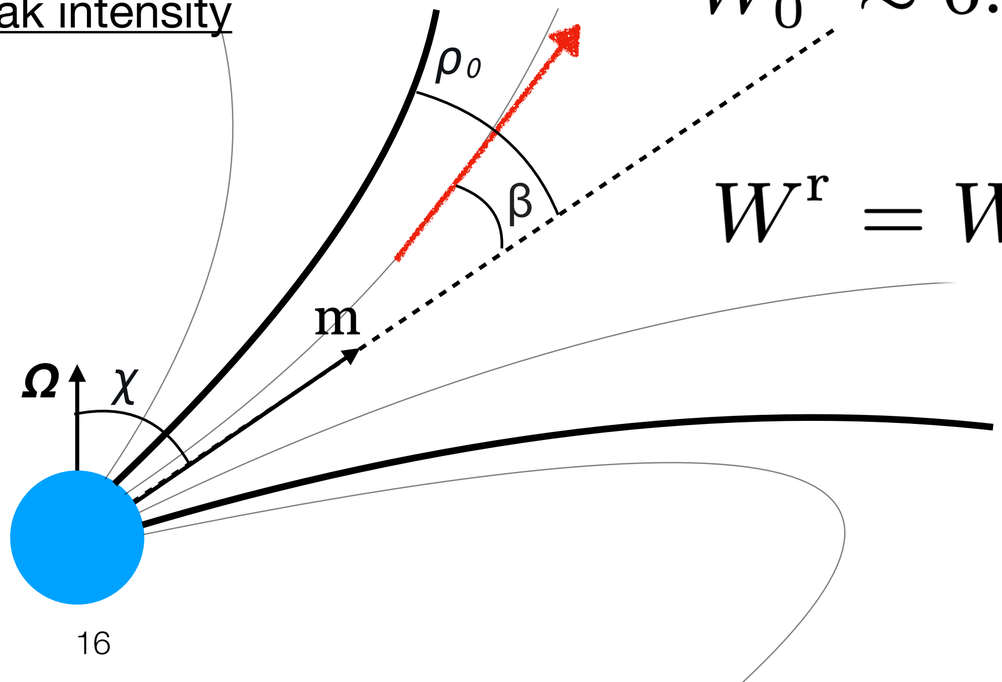

# Dependency on the pulsar period